UNIVERSITY OF BIRMINGHAM

UF
UNIVERSITY of FLORIDA

Simulation investigation of mode hopping in the H1 signal recycling cavity

Paul Fulda, Daniel Brown, Charlotte Bond, Kiwamu Izumi, Lisa Barsotti and Andreas Freise

LIGO DCC: T1500230

Issue: 2
Date: June 4, 2015

School of Physics and Astronomy
University of Birmingham
Birmingham, B15 2TT

University of Florida
Department of Physics
Gainesville, FL32611-8440

Contents

1 Introduction

During commissioning of the H1 dual-recycled Michelson interferometer (DRMI), the signal recycling cavity (SRC) was observed to exhibit the phenomenon known commonly as *mode-hopping* [1].

In the context of optical cavities, this phenomenon typically occurs when the length/frequency error signal has several nearby zero crossings, usually corresponding to resonances of different spatial modes of the cavity. External perturbations of the cavity length may cause the lock to 'hop' between two or more of these spatial mode resonances. Unmitigated mode hopping in the SRC is a major concern chiefly because it leads to DRMI lock losses. If mode hopping occurs during full interferometer operation, the duty cycle will be affected even without considering lock losses, however, because only data segments when the SRC is locked on the HG_{00} mode provide useful strain data.

Soon after the mode hopping was observed in the H1 DRMI it was indicated that the hopping frequency was dependent the alignment state of the central interferometer. In general, better initial alignment led to a reduced amount of mode hopping [3]. Further evidence for this was provided when the alignment sensing and control (ASC) loops were engaged and the mode hopping ceased [4].

This note summarises a simulation investigation into the mode hopping problem in the aLIGO SRCs. Finesse simulations of the H1 and L1 DRMIs were compared with the experimental observations in order to better understand the important variables which determine the hopping state, and with the aim of providing solutions for mitigating the problem. Up to date Finesse files for the H1 FPDRMI with DARM offset can be found at [2]

2 Tuning DRMI and length sensing matrix

The first stage of the simulation investigation was preparation and verification of the DRMI Finesse simulation files. We start with an ideally mode matched DRMI, based on the optical parameters recorded in [5] and the

Parameter	Unit	Value
PRM Rc	m	-10.948
PR2 Rc	m	-4.543
PR3 Rc	m	36.021
SRM Rc	m	-5.715
SR2 Rc	m	-6.424
SR3 Rc	m	36.013
ITMX Rc	m	-1939.32
ITMY Rc	m	-1939.39
Length PRM to PR2	m	16.6128
Length PR2 to PR3	m	16.1626
Length PR3 to BS HR	m	19.5381
Length SRM to SR2	m	15.740
Length SR2 to SR3	m	15.4601
Length SR3 to BS AR	m	19.3661
Length BS AR to CPX	m	4.829
Length BS HR to CPY	m	4.847
Thickness of CPs	mm	100
Thickness of ITMs	mm	200
Distance from CPs to ITM HR	mm	20
Physical path length travelled in BS	mm	68.5
Schnupp asymmetry length	cm	9.49
PRC optical path length	m	57.656
SRC optical path length	m	56.008
ITM thermal lens focal length	km	34.5
f1 Sideband frequency	Hz	9099471
f2 Sideband frequency	Hz	45497335
SRM transmission	%	36.96

Table 1: Parameters used for the ideally mode matched H1 DRMI model.

optics locations recorded in [6]. The recycling cavities were designed for ideal mode matching to the arm cavities in the presence of a 34.5 km lens in the ITM substrate. The 34.5 km lens is the ITM thermal lens expected in full lock for an input power of 18 W to the PRM, with 0.5 ppm absorption on the ITM HR surface [7]. Several of the relevant parameters for the H1 DRMI model are presented in tab. 1.

Tuning the interferometer to the correct operating point was performed in two stages. In the first stage the carrier and sideband field amplitudes at various locations within the interferometer were used as indicators of the tuning state. The microscopic positions of the power recycling mirror (PRM) and the two ITMs were tuned such that the ±9 MHz and ±45 MHz sideband field components were resonant in the power recycling cavity (PRC), and that the Michelson transmission was at a minimum for the carrier light. In the DRMI case, the carrier is anti-resonant in the PRC while the sidebands are resonant, as opposed to the full interferometer (FPDRMI) case where all three frequency components are simultaneously resonant. The signal recycling mirror (SRM) was tuned such as to make the ±45 MHz field components resonant in the SRC, as per the DRMI length sensing and control (LSC) scheme [8]. The plots of the left hand column of figure 1 show the field amplitudes in appropriate locations for the tuning of the three relevant length degrees of freedom (DOFs) for the ideally matched H1 DRMI.

The next step was to define error signals for the DRMI length DOFs, and then tune the DRMI further such as to minimize the error signals. The error signals used for this process were the same as those reported in [1]: REFL9I for PRCL, REFL45Q for MICH and REFL45I for SRCL. Several iterations were required when tuning to minimize these error signals, primarily due to the appearance of the PRCL DOF in the SRCL error signal.

Table 2 shows the length sensing matrix obtained from the model after tuning the ideally mode matched DRMI. The DRMI sensing matrix is known to contain one large "off-diagonal" element, shown in tab. 2 in red. This element represents the coupling of the PRCL DOF into the REFL45I signal, nominally used for control of

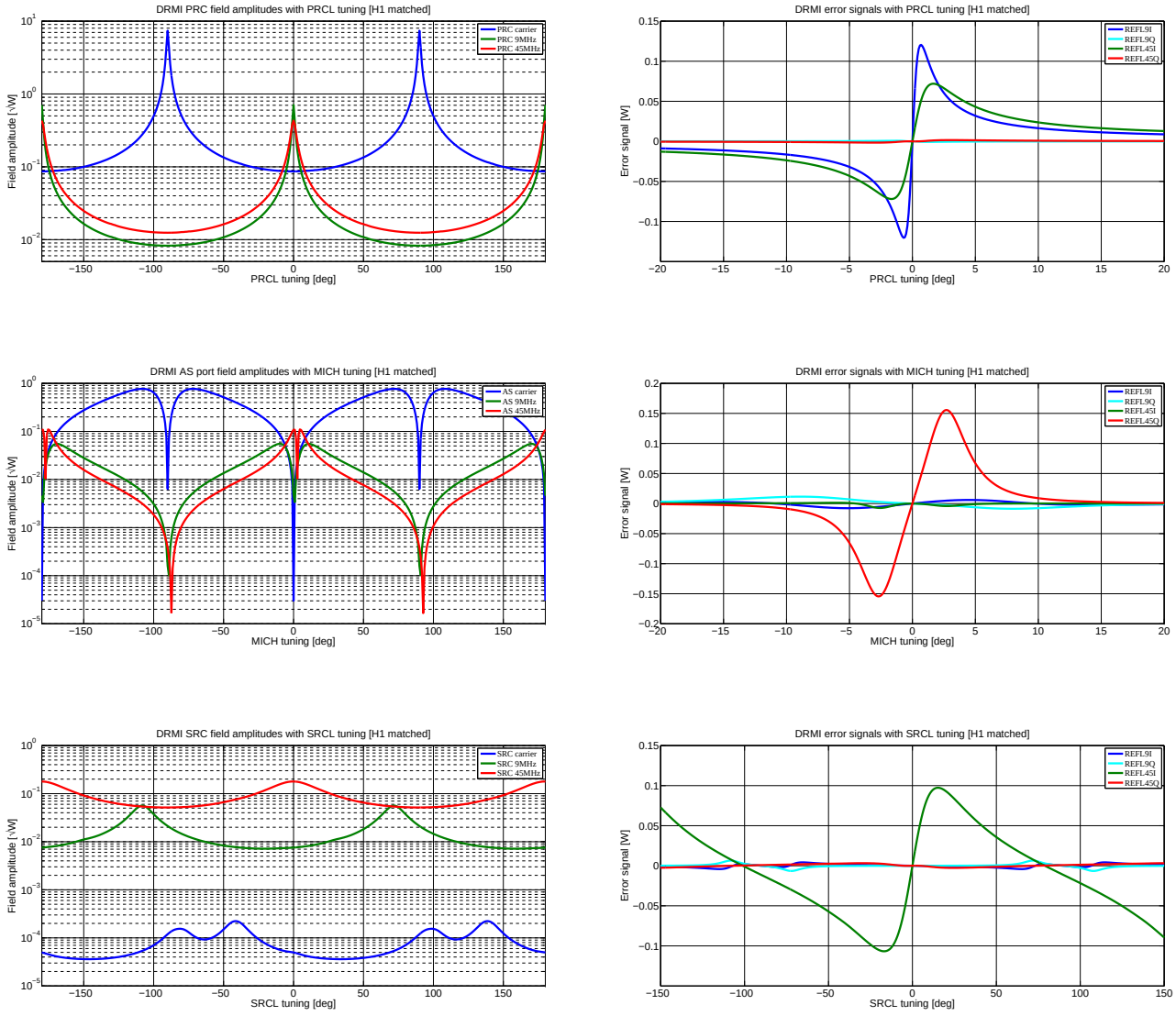

Figure 1: Field amplitudes (left column) and error signals (right column) for the PRCL (upper row), MICH (middle row) and SRCL (bottom row) degrees of freedom in the mode matched H1 DRMI.

the SRCL DOF. In order to avoid the SRCL DOF being swamped by motion of the PRCL DOF, the signal from the nominal PRCL sensor (REFL9I) is also fed forward to SRCL with the appropriate phase and amplitude in order to mitigate the effects of PRCL to SRCL coupling.

The optimal amplitude of the feed-forward correction of this cross-coupling can be measured and optimized by driving PRCL and adjusting the control matrix element for REFL9I→SRCL until this signal is minimized in REFL45Q [10]. The optimal feedforward amplitude has however been known to change in time in the H1 DRMI, although the cause is not well known. This should be kept in mind in the context of SRCL mode hopping, since the PRCL to SRCL cross coupling may be an additional source of SRCL motion that can lead to hops between SRCL error signal zero crossings. This idea is discussed further in section 5.

Port	PRCL	SRCL	MICH
REFL9I	1.037	0.000	0.006
REFL9Q	0.002	0.000	-0.003
REFL45I	0.255	0.037	-0.001
REFL45Q	0.001	0.000	0.200

Table 2: Length sensing matrix for the H1 ideally matched DRMI model. The blue elements represent the desired sensing element in that DOF column. The red element represents the unwanted "off-diagonal" element for coupling from PRCL to REFL45I (nominally the SRCL sensor). The gray elements are unused.

3 Effect of core optic alignment

3.1 Simulation

The effect of core optic alignments on the SRCL error signal was simulated using the ideally mode matched and tuned H1 DRMI model described in section 2. For each core optic tilt considered, the MICH and PRCL DOFs were held at their working points by an iterative locking procedure that adjusts the tuning of the DOF in order to bring the designated error signal to within a small specified range. This is essential in order to distinguish between the intrinsic effects of misalignment (e.g. HOM coupling) on the SRCL error signal, and the effects of geometric length offsets caused by changing the alignment of core optics on the SRCL error signal, for example via PRCL→SRCL coupling.

The results for pitch and yaw of the beam-splitter, ITMX and SR3 are shown in fig. 2. In these plots the SRCL error signal (REFL45I) is shown as a function of SRCL tuning offset, for a range of core optic tilt values. It can be seen that with increasing core optic tilt, the SRCL error signal becomes increasingly distorted from its initial shape. For a large enough tilt a second zero crossing usually appears in the SRCL error signal, which could lead to mode hopping behaviour similar to that observed in the H1 DRMI. The plots for the beam-splitter and ITMX look similar in that both show a feature at a negative detuning that eventually becomes a second and third zero crossing with enough misalignment, while leaving the tuning at which the intial zero crossing occurs relatively unchanged. In the SR3 case, however, the tuning at which the initial zero crossing occurs drifts significantly with increasing tilt. This is simply a result of the geometric coupling between alignment and length in a resonant cavity[1].

The process by which the SRCL error signal becomes distorted is clarified by fig. 3. In this figure, various carrier and 45 MHz HOM field components are shown as a function of SRCL detuning while either the beam-splitter or ITMX are misaligned in yaw by 0.4 μrad[2]. As the misalignment is increased, the proportion of circulating fields in the SRC in the HG_{10} mode relative to the HG_{00} mode increases, for both the carrier and 45 MHz field components. The HG_{10} mode can quickly dominate the carrier light in the SRC due to the high reflectivity of the Michelson for the HG_{00} carrier, as show in the left hand plots of figure 3.

In order to verify that in the simulation the two positive zero crossings in the SRCL error signal that appear in the presence of misalignment correspond to two different mode-hopping states, the AS port beam intensity profile was generated at the SRM tunings corresponding to these zero crossings. The results are shown in fig. 4, for the case where ITMX was misaligned in yaw by 0.4 μrad. As expected the intensity patterns show clearly that different modes dominate in the SRC and thus the AS port at each of the positive zero crossings: close to zero detuning from the aligned SRM tuning, the dominant mode appears to be HG_{00}, whereas at a detuning of -54 nm, corresponding to the misalignment induced positive zero crossing, the HG_{10} mode dominates.

What follows is an attempt at an intuitive explanation of the impact of misalignment of the beam-splitter or ITMs on the SRCL error signal: In the presence of a misalignment of either the beam-splitter or one of the ITMs, the Michelson interferometer converts HG_{00} modes to $HG_{10/01}$ modes in transmission into the SRC. This is because the lock on the MICH DOF ensures that the Michelson fringe is dark for the carrier HG_{00} mode, but differential misalignment between the light in the X and Y arms of the Michelson (such as is caused by beam-splitter or ITM misalignment) creates $HG_{10/01}$ modes which do not see a dark fringe for the Michelson.

[1] The same effect occurs for the PRC and to an extent the Michelson for tilts of PR3, ITMX etc., but in this simulation the iterative locks hold those DOFs at their working points and thus track the length changes from the geometric coupling with alignment.

[2] Adobe Reader viewers should see an animation where different time steps show different yaw tilt values up to 0.4μrad.

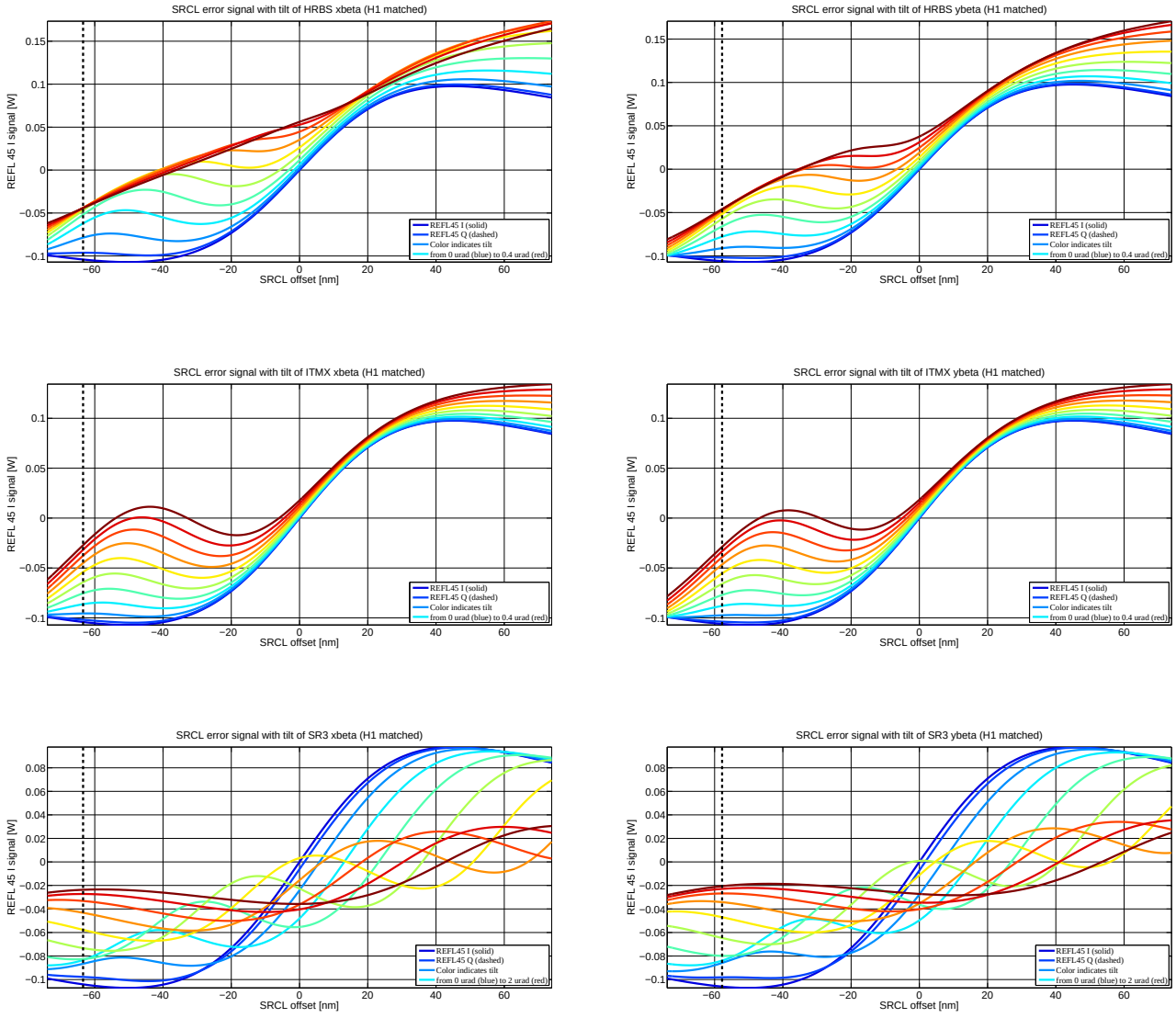

Figure 2: SRCL error signal (REFL45 I) as a function of SRCL detuning for a range of beam-splitter (upper row), ITMX (middle row) and SR3 (lower row) misalignments in yaw (left column) and pitch (right column). Misalignments of a few tenths of a microradian in the beamsplitter and ITMX, or about a microradian in the SR3, are enough to cause additional zero crossings in the SRCL error signal. The vertical black dashed line shows the resonant tuning of the SRC for the HG_{10} yaw mode (left column) and the HG_{01} pitch mode (right column), with the caveat that SR3 tilt affects the longitudinal tuning of the SRC resulting in a shifting resonant tuning of both HG_{00} mode and $HG_{10/01}$ modes.

The $HG_{10/01}$ modes therefore pass into the SRC, where they experience a different resonance condition than the HG_{00} mode due to the round-trip Gouy phase of the cavity. While this effect is more stark for the carrier field due to the strict dark fringe condition or the HG_{00}, it is also seen in fig. 3 to be significant for the 45 MHz sideband field, despite the lower reflectivity of the Michelson for the 45 MHz HG_{00} mode. When the $HG_{10/01}$ modes encounter the beam-splitter again from the SRC side, they are converted back into the HG_{00} mode by the reverse of the process that created them in the first place. However, the phase of these reconverted modes is different from the phase of HG_{00} modes which either never experienced the SRC at all (as in the carrier case), or experienced a different resonance condition from the modes which remained HG_{00} throughout (as in

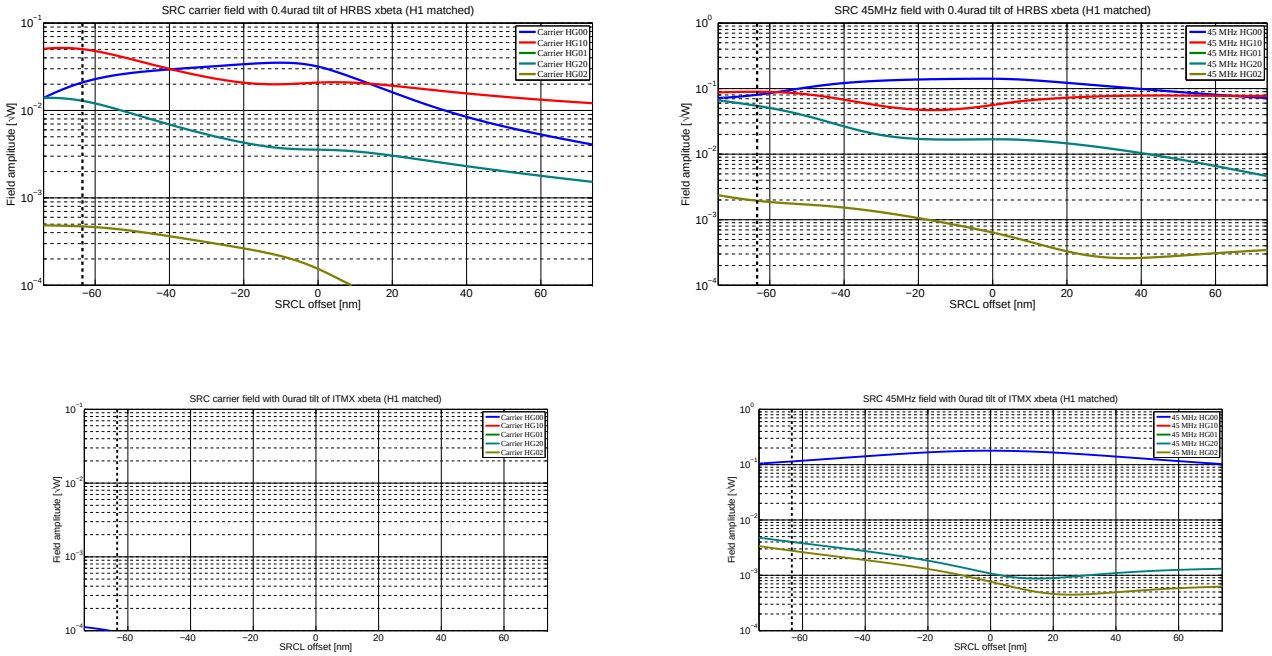

Figure 3: Carrier (left) and 45 MHz sideband (right) field components circulating in the SRC with yaw misalignment of beam-splitter (upper row), ITMX (middle row). Adobe Reader viewers: animation shows different yaw values up to 0.4 μrad.

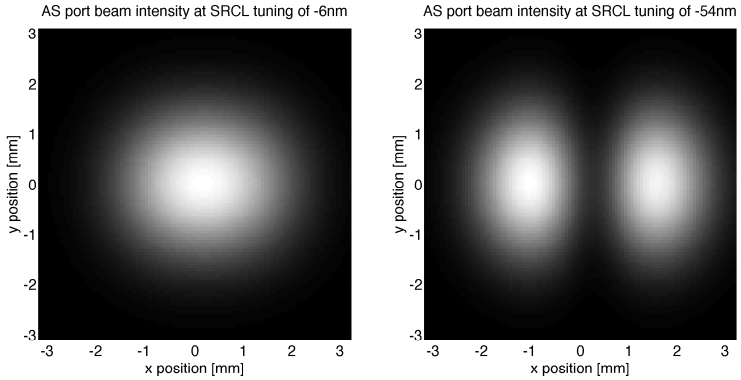

Figure 4: AS port intensity profiles for SRCL tunings corresponding to the two zero crossings identified in the SRCL error signal for an ITMX yaw of 0.40 μrad, as shown in the middle right plot of fig 2.

the 45 MHz case).

The error signal at REFL45I is a result of the beat between the carrier light and the 45 MHz sidebands in reflection from the Michelson. As such it is sensitive to a combination of all the different field components previously discussed. In the ideal case with no misalignments, the error signal arises purely from the beat of the

carrier HG_{00} mode, which is insensitive to the SRC tuning since it never passes into the SRC, and the 45 MHz sidebands, which do pass into the SRC and are nominally resonant there and thus have strong phase sensitivity to the SRC tuning. The complication added by misalignment arises due to several additional beat terms. The first of these addition beat terms is between carrier light which was converted into $HG_{10/01}$ modes in the SRC by the Michelson (and then back to HG_{00} in transmission from the SRC side of the Michelson back into the PRC side), and the 45 MHz light which remained in the HG_{00} mode throughout. The carrier light phase here is strongly sensitive to the SRC tuning **around the resonance condition of the $HG_{10/01}$ mode in the SRC**. The next additional beat term arises from the beat between carrier HG_{00} light which never makes it into the SRC and 45 MHz light which is converted to $HG_{10/01}$ modes in the SRC by the misaligned Michelson. Similar to the previous beat, this beat has a contributing component whose phase is sensitive of the SRC tuning around the resonance of the $HG_{10/01}$ mode in the SRC. The final, and probably least significant additional beat component arises between carrier light and 45 MHz light, both of which is converted to $HG_{10/01}$ modes in the SRC and back to the HG_{00} mode in the PRC by the misaligned Michelson.

As a result of all these additional beat terms having at least one contributing field which has phase sensitivity to the $HG_{10/01}$ mode resonance in the SRC, the total REFL45I error signal has sensitivity to the resonance of the $HG_{10/01}$ mode in the SRC as well as the HG_{00} resonance in the SRC. If the conversion factor for HG_{00} modes into $HG_{10/01}$ modes by the misaligned Michelson is large enough, this $HG_{10/01}$ mode sensitivity competes with the HG_{00} sensitivity, and the REFL45I error signal may acquire another zero crossing close to the resonance of the $HG_{10/01}$ mode, with the same sign as the zero crossing close to the resonance of the HG_{00} mode.

This is not unlike the extra zero crossings in PDH signals for a single cavity which may be seen for HOMs in the input beam. However, due to the low reflectivity of the SRM and the resulting low SRC finesse, the error signals have large linear ranges and the $HG_{10/01}$ and HG_{00} sensitive parts tend to blend together. The relative impact of the $HG_{10/01}$ mode resonances is also increased by the dark fringe condition of the Michelson for the carrier light, compared to the simple Fabry-Perot cavity case.

3.2 Comparison with observations

Observations of the H1 DRMI showed that the mode hopping was indeed strongly dependent on the alignment of the core optics. Once the WFS loops were adequately commissioned, it was possible to achieve a well aligned DRMI with the following procedure:

- Run the initial alignment procedure.
- Lock the DRMI length DOFs, with a positive offset on SRCL to avoid hopping regions.
- Engage WFS loops to optimize alignment.
- Remove SRCL offset.

After this procedure, the beam-splitter was tilted gradually until mode hopping was observed in the SRC, and the alignment offset values recorded. Similar measurements were repeated for several other core optics, as described in [11], and the results are summarized in tab. 3, along with the results from the simulations with an ideally mode matched H1 DRMI. For the optics whose misalignment led to mode hopping most rapidly, i.e. the beam-splitter and ITMX, the values from measurement and simulation agree well. For other optics, the measurement observed mode hopping at lower misalignment values than the simulation. This may be due to the effects of beam clipping at large misalignment angles in the measurement that were not accounted for in the simulation.

For the signal recycling cavity, it is reasonable to expect that the sensitivity of the mode hopping state to misalignment of a given optic scales roughly with the beam size at that optic. The results of the simulations roughly follow this rough rule-of thumb[3], as the beam sizes at SR3 : SR2 : SRM are roughly in the ratio 56 : 8.5 : 2.1, and the simulated required misalignments of SR3 : SR2 : SRM for hopping are in the ratio 1 : 7 : 56.

[3]The different Gouy phases at the different SR optics may also be expected to affect the contribution of the misalignment to the REFL45I error signal. SR3 and SR2 are at very similar Gouy phase locations, whereas SRM is about 20° different, hence the departure from the rule-of-thumb for this optic.

Optic name	Measured tilt before SRCL hopping occurs	Simulated tilt before second REFL45I zero crossing occurs
BS	$\pm 0.2\,\mu$rad	$\pm 0.22\,\mu$rad
ITMX	$\pm 0.4\,\mu$rad	$\pm 0.36\,\mu$rad
SR3	$\pm 0.5\,\mu$rad	$\pm 1.2\,\mu$rad
SR2	$\pm 4\,\mu$rad	$\pm 8.5\,\mu$rad
SRM	$\pm 16\,\mu$rad	$\pm 70\,\mu$rad

Table 3: Measured and simulated yaw offsets from ideal alignment required to cause mode hopping in the H1 SRC.

4 Effects of other interferometer variables

Although the misalignment of the core optics is expected to be the primary cause of the mode hopping in the H1 DRMI, it is also worthwhile to investigate other interferometer parameters which may determine the sensitivity of the SRCL error signal shape to these misalignments. One of the major motivations for this is the fact that observations at the H1 and L1 DRMIs show different situations with respect to mode hopping, even with similar misalignments of core optics, as is discussed further in section 6.

4.1 Mode matching

The simulations as described so far have all assumed perfect mode matching between the cavities that make up the DRMI. However, it is known that this mode matching varied over the course of the H1 DRMI commissioning as the thermal compensation system (TCS) was used to correct for mismatches initially present due to ITM substrate inhomogeneity lensing [12, 13] and also potential errors in the SR optics curvatures [14]. The mode matching states of the L1 DRMI and the H1 DRMI were also expected to differ because of these mode mismatches. The mode matching state of the DRMI was therefore identified as a possible factor which may determining whether any DRMI may experience mode hopping or not, because the H1 DRMI experienced mode hopping and the L1 DRMI did not.

We can distinguish between two different categories of mode mismatch which may play different roles in determining the hopping state of the DRMI: *common* mode mismatch and *differential* mismatch. In the DRMI both the PRC and the SRC are made up of two cavities; between P(S)RM and ITMX, and between P(S)SRM and ITMY. These four cavities are commonly referred to as PRX, PRY, SRX and SRY, where X/Y refers to the ITM which is probed by the beam within that cavity. Each of these four cavities can be traced to find specific eigenmodes. In the case where everything is symmetric from the beam-splitter to ITMX and ITMY, the PRX eigenmode and the PRY eigenmode are identical, as are the SRX and SRY eigenmodes. A *common* mode mismatch refers to case where PRX and PRY are the same, as are SRX and SRY, but PRX/Y and SRX/Y do not have the same eigenmodes. Such a situation may occur when, for example, the radius of curvature (RoC) of SR3 is changed from its nominal value. A *differential* mode mismatch refers to a case where the average PRX/Y eignenmode is equal to the average SRX/Y eignenmode, but the PRX and PRY eigenmodes are different to each other, as are the SRX and SRY eigenmodes.

The effects of common and differential mode mismatch on the DRMI can be quite different, due mainly to the dark fringe condition of the Michelson. Any differential mismatch converts the HG_{00} mode of the PRC to $HG_{20/02}$ modes in the SRC efficiently, as part of the dark fringe contrast defect. Common mismatch, on the other hand converts a smaller fraction of PRC HG_{00} modes to the SRC, since it does not affect the contrast defect. Instead, only light that was passing into the SRC anyway (primarily 45 MHz sidebands) is converted partially into the $HG_{20/02}$ modes by the common mismatch. Another important effect related to common mismatch is the change in SRC Gouy phase associated with a change in the SRC eigenmode. This affects the spacing of HOM resonances in the SRC, thus changing the impact of the alignment effects described in section 3 on the SRCL error signal.

4.1.1 Common SRC mode mismatch

In order to assess the impact of common SRC mismatch on the SRCL error signal, the simulation described in section 3 was extended to include a number of different SR3 RoC values, offset from the nominal 36.021 m.

The range of SR3 RoC offset values considered was between -2 cm and 2 cm: quite a conservatively large range relative to the expected uncertainties on the actual measured SR3 RoC. This range of SR3 RoC offsets gave a range of SRC round-trip Gouy phase values between about 55° and 25°, as shown in figure 5.

Figure 5: SRC round-trip Gouy phase as a function of SR3 RoC offset from nominal value of 36.021 m. The Gouy phase differs between x and y-axes because of the incident angle of the beam on the curved mirrors in the SRC.

Figure 6 shows the results of the simulation. The plots in fig. 6 show the SRCL error signal as a function of SRM tuning, with the different colored lines representing different SR3 RoC offset values. The SRM tunings which correspond to resonance of the HG_{10} or HG_{01} mode in the SRC are shown for several of the SR3 RoC offset values by the dashed vertical lines. Adobe Reader viewers will see an animated plot, where the time steps correspond to different alignment offset values. In the case where the viewing software does not show the animation, the plots should show a fixed misalignment value which still displays the main result.

In general, we see that for greater SR3 RoC offsets (corresponding to smaller SRC Gouy phase and therefore $HG_{10/01}$ mode resonances closer to the HG_{00} mode resonance) the error signal is less prone to the development of second positive zero crossings. This is understood as a blending together of the $HG_{10/01}$ phase sensitivity with the HG_{00} phase sensitivity of the SRCL error signal, to the point where they are no longer distinct enough to create sharp features such as second zero crossings. This is not to to say that the resulting error signal is not compromised in the case of low SRC Gouy phase. For low SRC Gouy phases, we in fact see a large shift in the SRM tuning at which the zero crossing occurs. It is likely that the zero crossing in these cases corresponds to some midway point between resonance of the $HG_{10/01}$ mode and the HG_{00} mode, in which case the interferometer operating point will still be far from the desired one.

A difference in SRC Gouy phase may help to explain the difference in observations at the two LIGO sites. If the SRC Gouy phase is lower in the L1 DRMI, rather than begin mode hopping with beam-splitter alignment, the SRC may in fact just incur an alignment dependent length offset. Intermediate SRC Gouy phase values offer even show another possible situation. For some SRC Gouy phase cases, certain beam-splitter the error signal flattens out at the zero crossing. The sensing gain for SRCL effectively drops to zero in this situation which will likely lead to lock loss, as is observed for beam-splitter misalignments above 0.2 μrad in the L1 DRMI.

4.1.2 Differential (XY) mode mismatch

In order to assess the effect of differential mode mismatch, i.e. a mismatch between the two arms of the interferometer, the simulation was performed again but this time for a range of different ITM substrate lens values. Since the common ITM substrate lens also has a strong effect on both PRC and SRC Gouy phases, the lenses in both ITMs were actuated differentially in order to distinguish from the common mode mismatch case. A positive lens was applied to ITMY, and a negative lens applied to ITMX.

As shown in fig/ 7 a purely differential ITM substrate lens causes a small change in the average Gouy phase of the SRC $(\Psi_{SRX} + \Psi_{SRY})/2$. This is because the effect of a negative lens on the Gouy phase increases as the SRC comes close to instability. Over the range of ITM differential lenses investigated (0 to 24μD), however, the change in average SRC Gouy phase was only about 6°. This is small compared with the $\tilde{3}0°$ range of SRC

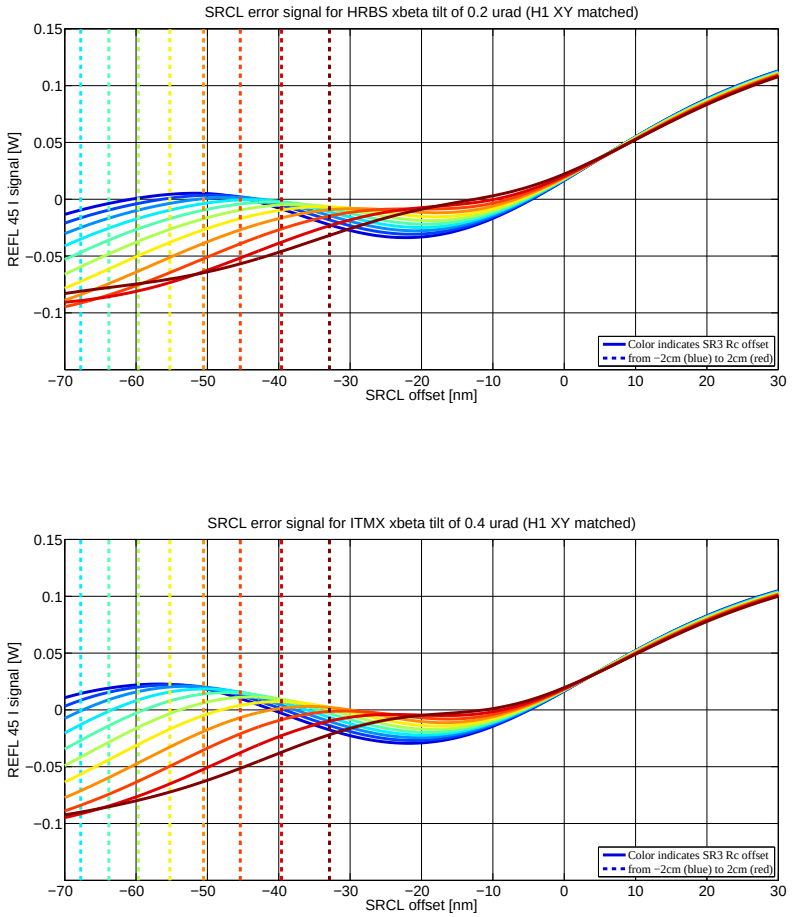

Figure 6: SRCL error signals as a function of SRCL detuning for a range of SR3 RoC offsets and a yaw misalignment of the beam-splitter of 0.2 μrad (upper plot) and a yaw misalignment of ITMX by 0.4 μrad (lower plot). Adobe Reader viewers: animation shows different yaw values up to 0.3 μrad for the upper plot, and up to 0.4 μrad for the lower plot.

Gouy phases investigated in the common mode mismatch case. If necessary, the lens powers aplied to ITMX and ITMY could be adjusted to give no change at all in the average SRC Gouy phase, while still maintaining a differential mode mismatch.

In fig. 8 it can be seen that in general, larger differential mode mismatches lead to an additional zero crossing appearing in the error signal at a lower core optic misalignment value. This is likely to be due to to the influence of the $HG_{20/02}$ modes in the SRC, into which the HG_{00} mode in the PRC is coupled via the differential mode mismatch of the two Michelson arms. This is very similar to the way in which the misalignment creates $HG_{10/01}$ modes in the SRC, the presence of which distorts the SRCL error signal. The differential mode mismatch produces a constant distortion in the SRCL error signal, which leads to a situation where a smaller distortion produced by misalignment is required to generate a second zero crossing in the error signal.

Note the difference in results for ITMX and ITMY misalignment: for larger differential mode mismatches the SRCL error signal is more sensitive to misalignments of ITMX than ITMY. This is due to the fact that SRX has a smaller Gouy phase than SRY when the differential lens is applied, because the lens in ITMX is negative. In general, a cavity with smaller Gouy phase has a larger geometric coupling from optic tilt to cavity axis tilt, and thus tilts of the ITMX with a negative lens cause larger couplings to $HG_{10/01}$ modes, and hence larger distortions in the SRCL error signal.

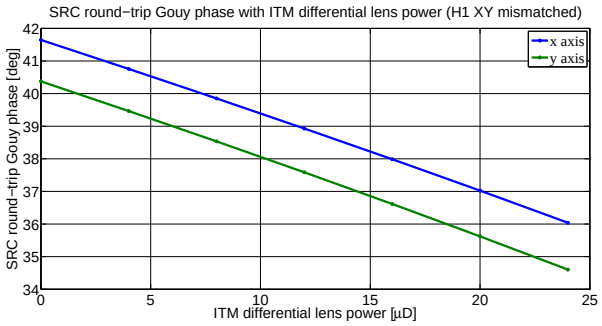

Figure 7: SRC round-trip Gouy phase as a function of differential ITM substrate lens. The Gouy phases plotted are the average values for SRX and SRY, where ITMX has an increasingly positive lens and ITMY has an increasingly negative lens.

4.2 Schnupp asymmetry length

The Schnupp asymmetry length was identified as another possible variable which determines the vulnerability of the SRC to mode hopping effects. This asymmetry length defines the reflectivity of the Michelson for the 45 MHz sidebands, as shown in figure 9. The Schnupp asymmetry length is ideally designed for critical coupling of the 45 MHz sideband into the SRC, that is to say that the reflectivity of the Michelson for 45 MHz is designed to be equal to the SRM reflectivity. However, the precision of the placement of optics was such that it was not unreasonable to assume an uncertainty in the actual Schnupp asymmetry length of a few cm.

Figure 10 shows the results of a simulation where the Schnupp asymmetry length was varied by ± 3 cm, as the beam-splitter or ITMX were misaligned. Here it can be seen that in general the longer the Schnupp asymmetry length, the more insensitive to misalignment the SRCL error signal becomes. For longer Schnupp asymmetry lengths, a larger misalignment was required to produce additional SRCL error signal zero crossings. In addition, the longer the Schnupp asymmetry length is, the more insensitive the original SRCL error signal zero crossing tuning is.

This can be understood by considering the reflectivity of the Michelson interferometer for the different field components as a function of Schnupp asymmetry length. As was discussed previously, misalignments of the core optics cause efficient coupling of HG_{00} modes in the PRC into $HG_{10/01}$ modes in the SRC. The Michelson is effectively fully transmissive to these modes, acting only to convert between modes. The $HG_{10/01}$ modes in the SRC are responsible for causing the distortions to the SRCL error signal, by adding additional beat terms that are sensitive to the $HG_{10/01}$ phase in the SRC.

To first order, the reflectivity of the Michelson for the $HG_{10/01}$ modes does not depend on the Schnupp asymmetry length. The Michelson reflectivity for the 45 MHz HG_{00} mode, however, does depend strongly on the Schnupp asymmetry length. The dominance of the desired beat term that is sensitive to the 45 MHz HG_{00} phase in the SRC over the spurious beat terms from the $HG_{10/01}$ modes is therefore dependent on the Schnupp asymmetry, since this determines the Michelson reflectivity and therefore the criticality of coupling and buildup for the 45 MHz HG_{00} mode.

4.3 SRM reflectivity

The SRM reflectivity is a variable that can possibly be tuned in order to mitigate the mode hopping problem, although there are likely to be other factors, such as broadband sensitivity in science mode, which may take precedence. The mode hopping problem in the DRMI is now known to originate from the influence of higher-order spatial modes in the SRC on the SRCL error signal. Higher-order mode effects can have significant influence on the SRCL error signal in part because the SRC finesse is so low that the influence of HOMs is not confined to a small region of SRCL tunings around their resonance. It was therefore considered possible that a higher SRM reflectivity, and thus higher SRC finesse, might mitigate the mode hopping problem by confining

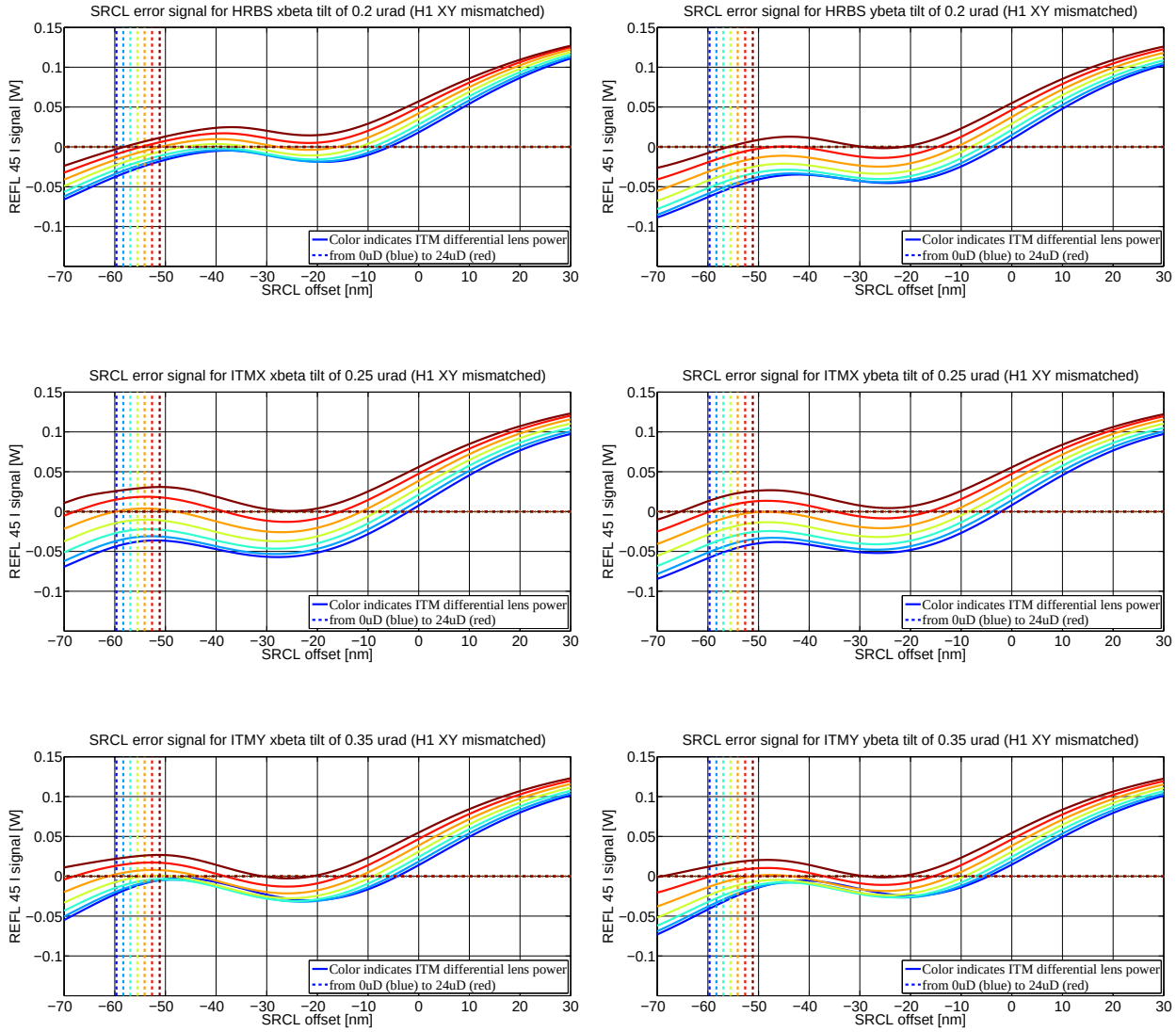

Figure 8: SRCL error signals as a function of SRCL detuning for a range of differential ITM differential lens values, and yaw/pitch misalignment of the beam-splitter of 0.2 μrad (upper row), yaw/pitch misalignment of ITMX by 0.25 μrad (middle row), and yaw/pitch misalignment of ITMY by 0.35 μrad (lower row). The dashed vertical lines indicate the average resonant tuning of the $HG_{10/01}$ mode for yaw/pitch, and the dashed horizontal lines show the REFL 45 Q signal. Adobe Reader viewers: animation shows different yaw values up to 0.3 μrad for the upper row, and up to 0.4 μrad for the middle and lower rows.

the HOM effects to a smaller region, away from the HG_{00} mode operating point.

Figure 11 shows the SRCL error signal as a function of SRM tuning for a range of core optic misalignments, similarly to fig 2 except this time for a range of different SRM transmissions. Here it can be seen that the effect of a lower SRM transmissivity is to narrow the linear range of the SRCL error signal, as expected. However, we also see that the influence of the HG_{10} mode on the error signal is still significant, and can still lead to a second positive zero crossing. A caveat here is that the ideal Schnupp asymmetry length does depend to an extent on the SRM transmission, as the Michelson reflectivity for critical coupling depends on the SRM transmission. In order to more fully explore the effects of different SRM reflectivities, one would have to also compare over a range of Schnupp asymmetry lengths.

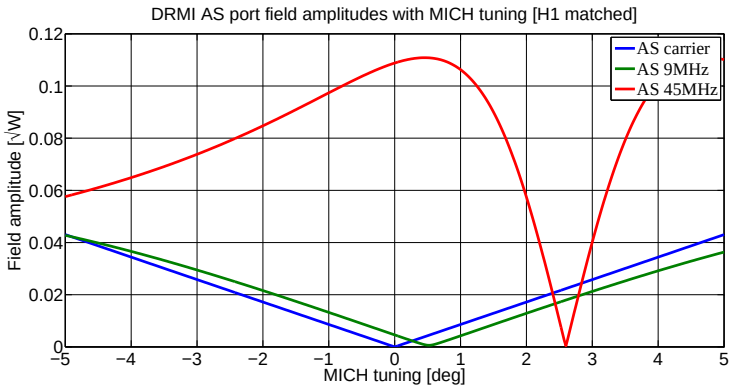

Figure 9: Field amplitudes at the AS port as a function of MICH tuning. The 45 MHz field amplitude at 0° detuning is dependent on the Schnupp asymmetry length. The MICH tuning separation of the minima in carrier and 45 MHz fields changes by about 0.27° per cm Schnupp asymmetry length.

4.4 Signal recycling cavity length

The length of the SRC determines the relative resonance conditions of the carrier and RF sidebands in the SRC. In DRMI operation, the carrier and 45 MHz light are expected to be co-resonant in the SRC. However, since the Michelson is at a dark fringe for the carrier light, the SRC is effectively a hugely undercoupled cavity for the carrier light. Little carrier light in the HG_{00} mode therefore makes it into the SRC, and therefore the effect of resonance/antiresonance on the carrier light is minimal. This is in contrast to the full FPDRMI operation with DC readout: in this case an small offset on the differential arm length (DARM) degree of freedom allows a significant portion of carrier light to enter the SRC. The (anti-)resonance condition of the SRC for the carrier therefore plays an important role, in particular in determining the interferometer gravitational wave transfer function.

The length of the SRC might not therefore be expected to play an important role in determining the DRMI mode hopping state, since the SRCL error signal should be insensitive to effect of SRC length change. which is to change the relative resonance conditions of carrier and 45 MHz sidebands in the SRC.

In order to verify this, the simulation was run for a range of different SRC length offsets, and for misalignments of the beam-splitter and ITMX. The results of this simulation are shown in figure 12. Here we see that over the range of macroscopic SRCL offsets considered (±2cm SRC offset), and the beam-splitter and ITMX misalignments, the SRCL error signal exhibits only very minimal dependence on the macroscopic SRC offset.

One thing to bear in mind with this particular simulation is the fact that the optimal demodulation phase for the REFL 45 I signal is dependent to some extent on the macroscopic length of the SRC. A preliminary observation of the error signals showed that over the range considered, the change in optimal demodulation phase does not significantly affect the results. The dashed lines in fig. 12 shows the REFL 45 Q signal, which remains null over the range of SRC offsets considered. However, the fact that the REFL 45 Q signal remains null does not necessarily indicate that the optimal demodulation phase is unchanged over the range of macroscopic SRC lengths, because the REFL 45 Q signal is driven to zero by the iterative lock applied to the PRCL degree of freedom. In order to assess the change in optimal demodulation phase, it is necessary to observe changes in the *sensing matrix* over the range of considered macroscopic SRC length offsets.

5 PRCL to SRCL sensing element alignment dependence

As was mentioned earlier in section 2, there is a strong coupling from the PRCL degree of freedom to the signal used for sensing the SRCL degree of freedom, REFL 45 I. In fact, as is shown in tab. 2, REFL 45 I is about 7 times more sensitive to PRCL than it is to SRCL. This effect is accounted for in the experiment by also feeding

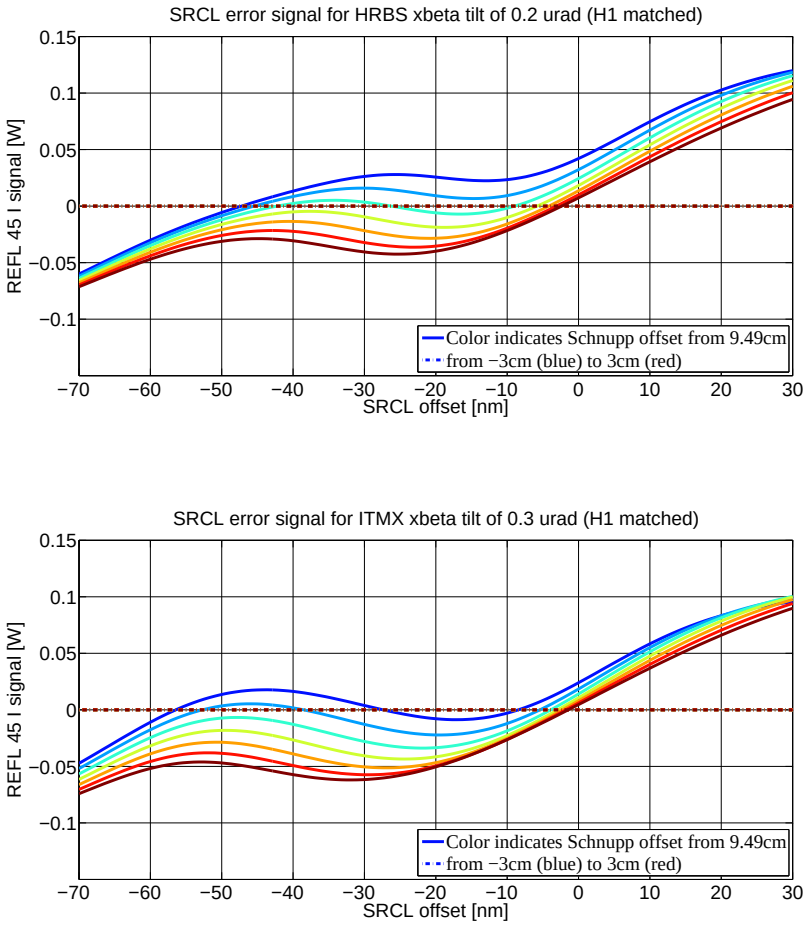

Figure 10: SRCL error signals as a function of SRCL detuning for a range of differential Schnupp asymmetry length offsets and a yaw misalignment of the beam-splitter of 0.2 μrad (upper plot), or a yaw misalignment of ITMX by 0.3 μrad (lower plot). The dashed horizontal lines show the REFL 45 Q signal. Adobe Reader viewers: animation shows different yaw values up to 0.3 μrad for the upper plot, and up to 0.4 μrad for the lower plot.

forward the PRCL error signal (REFL 9 I) to the SRCL degree of freedom, with appropriate amplitude and phase such as to cancel out the effect of the PRCL to REFL 45 I coupling. If, however, the ideal amplitude and phase of the feedforward should change, this cancellation will no longer be perfect and the PRCL degree of freedom will once again couple into the SRCL degree of freedom.

The effect of a change in PRCL on the SRCL error signal, in the event of imperfect feedforward of REFL 9 I to SRCL, will be to add an offset, pushing the whole SRCL error signal as shown for example in fig. 3. For many of the situations investigated throughout this note, a small time varying offset in the SRCL error signal could easily lead to hops between zero crossings.

6 Expected parameter space and conclusions

We have seen from the results in the previous section that there are several interferometer variables that can affect the likelihood of mode hopping in the aLIGO DRMIs. The simple observation from the two sites was that the H1 DRMI experienced hopping, whereas the L1 DRMI did not. Other more detailed observations from the H1 DRMI included the measurements of the required core optic misalignment to cause hopping, as shown in tab. 3. The only equivalent measurement from the L1 DRMI was the observation that at similar

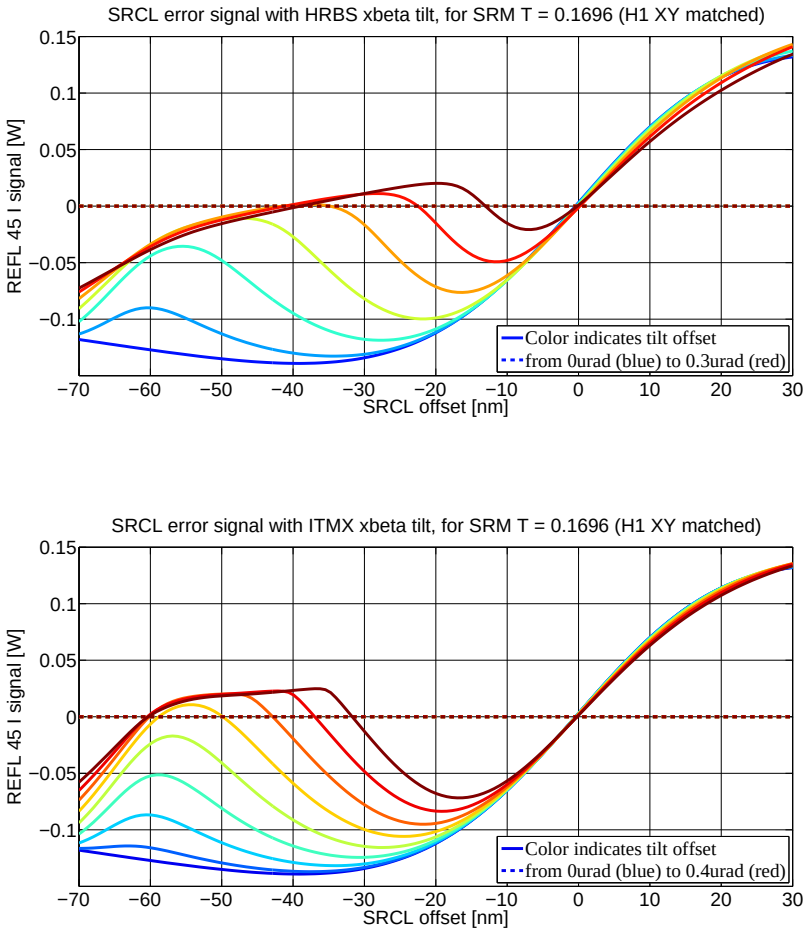

Figure 11: SRCL error signals as a function of SRCL detuning for a range of beam-splitter (upper plot), and ITMX (lower plot) yaw misalignments, with a lower SRM transmission of 17 %. Adobe Reader viewers: animation shows different SRM transmission values.

core optic misalignments to the those required to cause mode hopping in the H1 DRMI, the L1 DRMI would lose lock altogether. In this section, we attempt to gather information from the sites about the likely values of these variables, and thereby seek to explain the mode hopping observations (or non-observations) at the two sites.

Alignment. There is no reason to expect that either the initial alignment or the in-loop residual misalignment is significantly different for either DRMI. This is the primary reason that we have investigated other factors which can increase the susceptibility of the SRCL error signal to misalignments.

Common mode mismatch. Due to the possibly uncompensated ITM substrate inhomogeneity lenses, as well as the uncertainties in RoCs and positions of the SR optics (most notably SR3) at both sites, the common mode mismatch and therefore SRC Gouy phase is a variable which may explain the differences between sites. However, this variable is very difficult to measure, primarily due to the low SRC finesse. This remains something of a free parameter therefore in attempting to understand the behavior of the two DRMIs.

Differential mode mismatch. DRMIs at both sites have had the differential mode mismatch minimized by use of the TCS CO_2 laser [13, **?**]. We therefore do not expect the differential mode mismatch to play a significant role in explaining the difference between H1 and L1 DRMI mode hopping behavior.

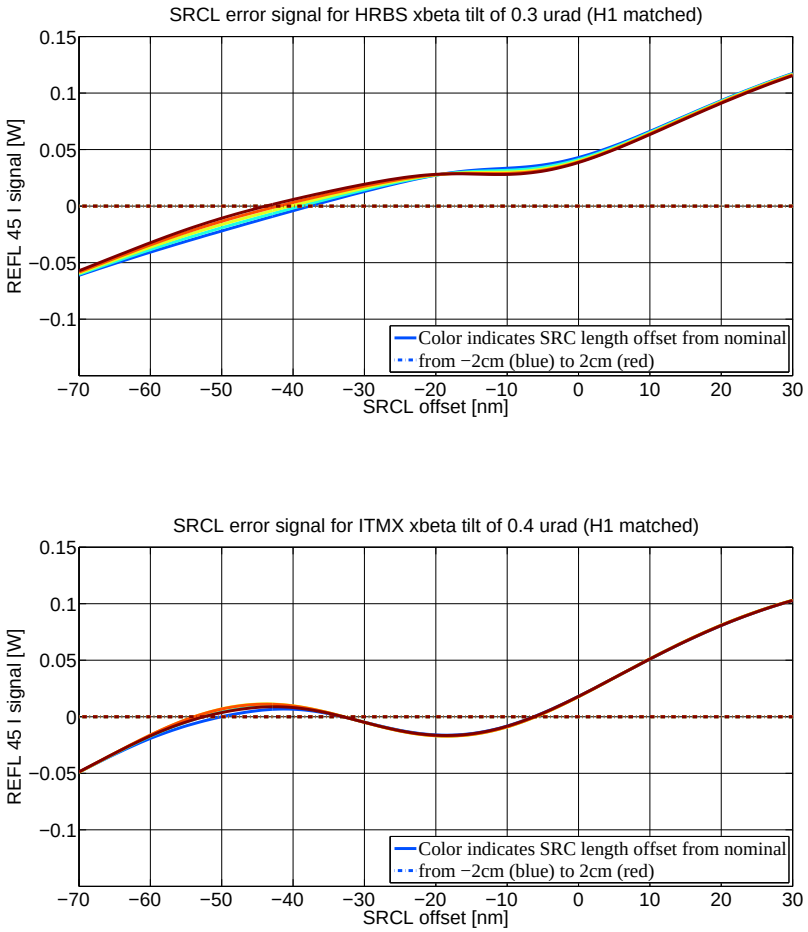

Figure 12: SRCL error signals as a function of SRCL detuning for a range of macroscopic SRC length offset values, and yaw misalignment of the beam-splitter of 0.3 μrad (upper plot), and yaw misalignment of ITMX by 0.4 μrad (lower plot). Adobe Reader viewers: animation shows different yaw values up to 0.3 μrad for the upper plot, and up to 0.4 μrad for the lower plot.

Schnupp asymmetry length. The Schnupp asymmetry lengths at the two sites are expected to have slightly different Schnupp asymmetry lengths. The most recent measurement of the H1 Schnupp asymmetry length gave the value of 8.9 cm [15], whereas the most recent measurements of the L1 Schnupp asymmetry gave the value 8 cm [16]. Simulations such as those shown in fig. 10 showed that a 1 cm change in Schnupp asymmetry length could affect the mode hopping situation with a reasonable significance. On the other hand, longer Schnupp asymmetry lengths tended to imbue the DRMI with a decreased sensitivity to misalignment. This is somewhat contrary to the observation that the H1 DRMI experienced mode hopping, whereas the L1 DRMI did not. Having said that, it is possible that an even more severe mode hopping situation at the L1 DRMI may simply manifest itself as the observed lock losses when the core optic misalignments were large.

SRM reflectivity. While the SRM reflectivity may be an important factor in determining the likelihood of the occurrance of mode hopping in the DRMI, this is not a variable which is expected to differ significantly between the two sites. The effects of the SRM reflectivity should be borne in mind in future, however, when switching to a new SRM reflectivity, for example for broadening the RSE response.

Variable	Effect on hop likelihood	Suggested fix
Core optic alignment	Misalignment of core optics causes second zero crossings in the SRCL error signal, which can lead to mode hopping.	Optimize initial alignment of DRMI, as well as optimizing DRMI ASC loops.
Common mode mismatch	Common mismatches which lead to smaller SRC Gouy phases reduce the hop likelihood, but at the expense of making the desired HG_{00} zero crossing strongly alignment dependent.	Not a viable variable for fixing the mode hopping problem. SRC should ideally be matched to CARM in FPDRMI.
Differential mode mismatch	Differential mismatches cause increased likelihood of mode hopping, due to the influence of $HG_{20/02}$ modes in the SRC on the SRCL error signal.	The differential mismatch should be minimized, with the use of the TCS CO_2 lasers and/or the ITM ring heaters.
Schnupp asymmetry length	Larger Schnupp asymmetry lengths cause decreased likelihood of mode hopping, for the SRM transmission chiefly considered (37%).	If SRM transmission is maintained at 37%, extend the Schnupp asymmetry length by 3 cm.
PRCL to SRCL coupling	Unmitigated PRCL to SRCL coupling will make hopping more likely, in the event that other variables lead to a situation where multiple zero crossings occur.	Include PRCL to SRCL coupling minimization as part of the initial DRMI lock acquisition procedure.
SRM reflectivity	Unclear due to variation in ideal Schnupp asymmetry length with SRM reflectivity. Expectation is that with well tuned Schnupp asymmetry, higher SRM reflectivity will lead to lower hop likelihood.	Increase SRM reflectivity, though this will likely be more strongly determined by other factors in the operation of aLIGO.
SRC length	Probably has a minimal effect on the mode hopping likelihood in DRMI operation.	Not a viable solution for the mode hopping problem. SRC length should ideally be determined by the resonance/anti-resonance condition of carrier and sidebands in FPDRMI operation.

Table 4: Summary of the effects of variables investigated, and how they might be used to mitigate the mode hopping problem in the aLIGO DRMIs.

SRC macroscopic length. In the simulations, this variable was not shown to have a significant effect on the SRCL error signal in the DRMI. Therefore we do not expect differences in the H1 and L1 DRMI macroscopic SRC lengths to contribute significantly to the different mode hopping observations at the two sites.

7 Strategies for mitigating the impact of mode hopping

Given the range of interferometer variables whose effects on the SRCL error signal has been studied, we may now attempt to identify some possible strategies for mitigating or eliminating the mode hopping problem from the aLIGO DRMIs. Table 4 shows a brief assessment of each variable investigated, along with a brief discussion of the potential of adjusting this variable to mitigate the mode hopping problem.

From this table of variables, there seem to be two that offer the most promise for mitigating or eliminating the mode hopping problem. First of all, simply improving the alignment of the core optics which comprise the DRMI will greatly mitigate the problem. All of the auxiliary variables investigated in the work described in this note have been analyzed in terms of their effect on the sensitivity of the SRCL error signal to misalignment. Alignment of the DRMI is therefore in some way the zeroth order improvement that can be made. There are

two aspects of DRMI alignment that should be optimized: initial alignment and closed-loop ASC. Discussing the details of improvements in the initial an in-loop alignment optimization is beyond the scope of this note, however.

References

[1] LHO aLOG 14002, Kiwamu Izumi et al., 09.18.2014,
https://alog.ligo-wa.caltech.edu/aLOG/index.php?callRep=14002 1, 2

[2] LIGO-T1300904,'Finesse input files for the H1 interferometer',
P. Fulda et al., 05.08.2015, https://dcc.ligo.org/LIGO-T1300904 1

[3] LHO aLOG 14027, Sheila Dwyer et al., 09.18.2014,
https://alog.ligo-wa.caltech.edu/aLOG/index.php?callRep=14027 1

[4] LHO aLOG 14394, Sheila Dwyer et al., 10.10.2014,
https://alog.ligo-wa.caltech.edu/aLOG/index.php?callRep=14394 1

[5] LIGO optics database https://galaxy.ligo.caltech.edu/optics/ 1

[6] LIGO-E1200616, 'H1 IO Master coordinate list', Luke Williams, 09.14.201,
https://dcc.ligo.org/LIGO-E1200616 2

[7] LIGO-T0900043, 'Optical Layout and Parameters of the aLIGO Recycling Cavities',
Muzammil Arain et al., 03.16.2012, https://dcc.ligo.org/LIGO-T0900043 2

[8] LIGO-T1000298, 'Advanced LIGO Length Sensing and Control Final Design', 09.04.2012,
Rich Abbott et al., https://dcc.ligo.org/LIGO-T1000298 2

[9] LHO aLOG 14492, Sheila Dwyer et al., 10.16.2014,
https://alog.ligo-wa.caltech.edu/aLOG/index.php?callRep=14492

[10] LHO aLOG 15362, Evan Hall et al., 01.12.2014,
https://alog.ligo-wa.caltech.edu/aLOG/index.php?callRep=15362 3

[11] LHO aLOG 15362, Evan Hall et al., 01.12.2014,
https://alog.ligo-wa.caltech.edu/aLOG/index.php?callRep=15362 7

[12] LIGO-T1300954, 'Investigation of beam clipping in the Power Recycling Cavity of Advanced LIGO using FINESSE', 12.05.2013,
Charlotte Bond et al., https://dcc.ligo.org/LIGO-T1300954 8

[13] LLO aLOG 9733, Chris Mueller et al., 11.15.2013,
https://alog.ligo-la.caltech.edu/aLOG/index.php?callRep=9733 8, 15

[14] LIGO-G1300909, 'Mode matching investigations at LLO',
Lisa Barsotti and Chris Mueller, 09.06.2013, https://dcc.ligo.org/LIGO-G1300909 8

[15] LHO aLOG 16851, David Ottaway et al., 02.22.2015,
https://alog.ligo-wa.caltech.edu/aLOG/index.php?callRep=16851 16

[16] LLO aLOG 8562, Lisa Barsotti and Denis Martyniv, 09.02.2013
https://alog.ligo-la.caltech.edu/aLOG/index.php?callRep=8562

16